Matos et al., http://www.jcb.org/cgi/content/full/jcb.201506025/DC1

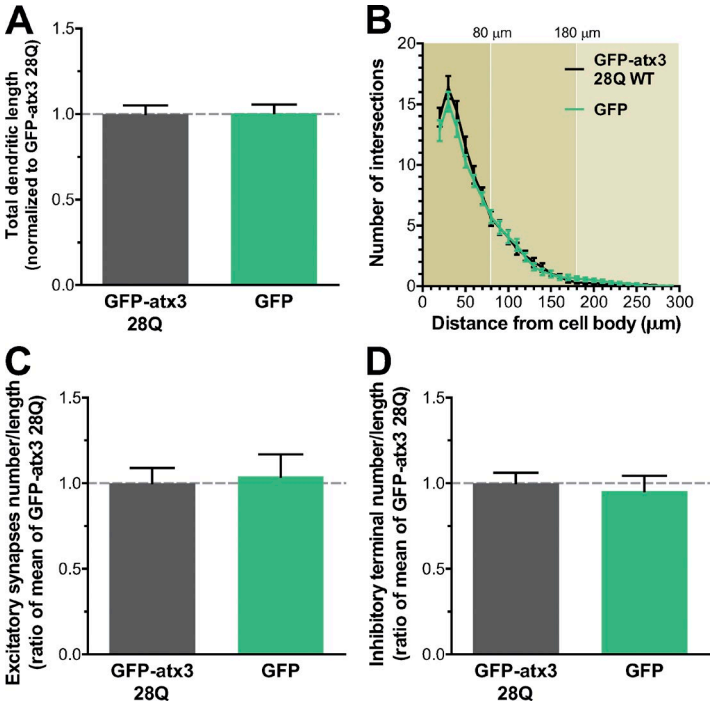

Figure S1. **Nonexpanded GFP-atx3 causes no neuromorphologic anomalies in transiently transfected cortical neurons.** Rat cortical neuron cultures were transfected with GFP-atx3 28Q or the empty pEGFP-C1 vector (GFP). (A) Neurons expressing GFP-atx3 28Q WT display no differences regarding total dendritic length (n = 42–47 neurons, from four independent experiments; t test: $P > 0.9$) or the dendritic arborization profile (B) as evaluated by Sholl analysis (n = 42–47 neurons, from four independent experiments; t test: $P > 0.05$). (C) No differences relative to the number of excitatory synapses (n = 38–40 neurons, from four independent experiments; t test: $P > 0.8$) or (D) inhibitory postsynaptic terminals (n = 35–34 neurons, from three independent experiments; t test: $P > 0.6$), were detected. (A–D) Graph bars represent mean ± SEM.

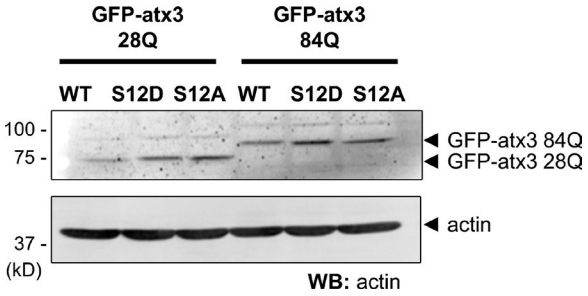

Figure S2. **Transfection of rat cortical neurons with GFP-atx3 phosphomutants.** Cultured rat cortical neurons with 9–10 DIV were transfected with GFP-atx3 28Q WT, GFP-atx3 84Q WT, or the respective S12D or S12A mutants, and 5 d later whole-cell lysates were analyzed by Western blot with an anti-GFP and an antiactin antibody. The differences in electrophoretic movement between GFP-atx3 28Q and GFP-atx3 84Q reflect the differences in molecular size resulting from the distinct number of glutamine residues.

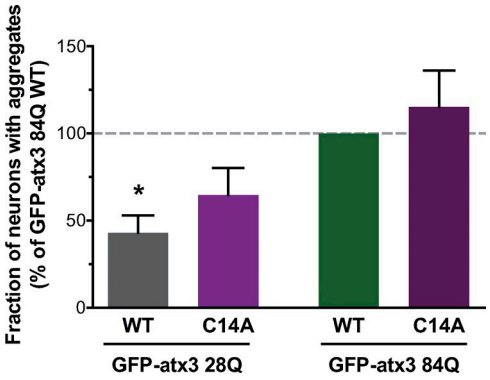

Figure S3. **DUB activity blocking causes no change on expanded atx3 aggregation in cortical neurons.** Transfection with the DUB inactive mutant GFP -atx3 84Q C14A yields a fraction of neurons with aggregates comparable with what is obtained on transfection with GFP-atx3 84Q WT (50–55 neurons counted for each condition in $n = 7$ independently prepared cultures; graph bars represent mean ± SEM; one-sample t test: *, $P < 0.05$).

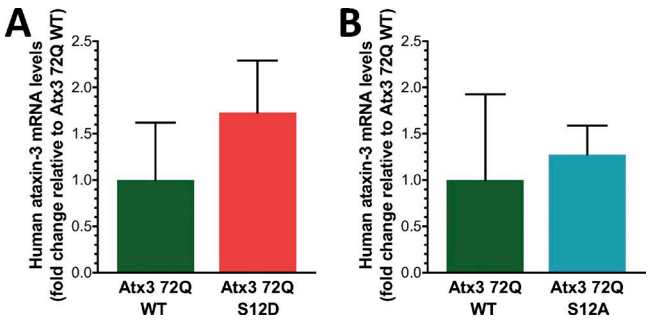

Figure S4. **Expression levels of atx3 72Q in the striatum of the MJD lentiviral rat models.** (A and B) RT-PCR analysis of human atx3 mRNA levels revealed no significant differences between brain hemispheres ($n = 3$ animals injected with atx3 72Q WT:atx3 72Q S12D or atx3 72Q WT:atx3 72Q S12A; graph bars represent mean ± SEM; Mann-Whitney test: $P > 0.05$).

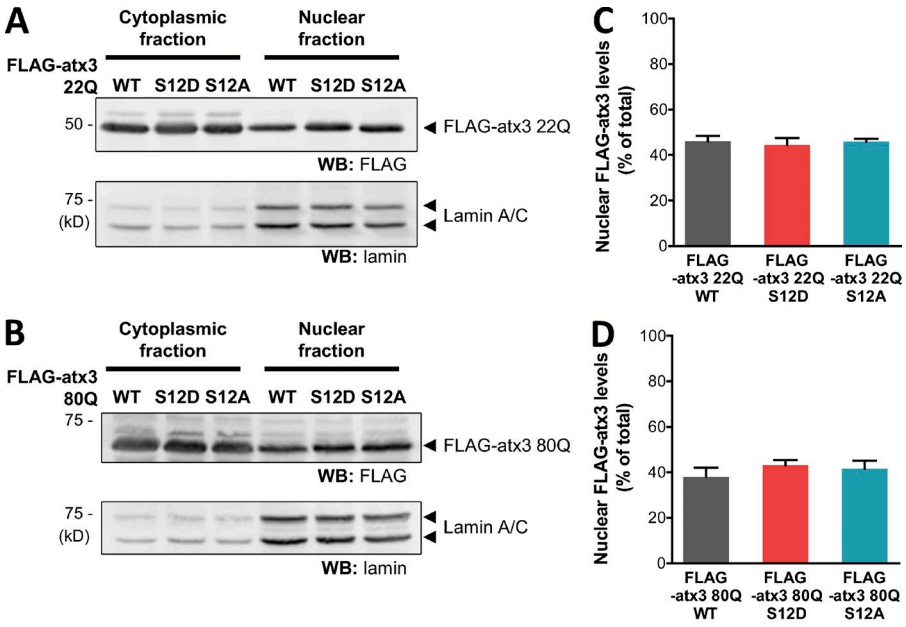

Figure S5. **Mutating S12 does not alter the nuclear accumulation of atx3, in COS-7 cells.** (A and B) COS-7 cells were transiently transfected with nonexpanded (22Q) or expanded (80Q) forms of WT and phosphomutated FLAG-atx3. Cell extracts were subjected to a nuclear fractionation procedure and the resulting cytoplasmic and nuclear fractions were analyzed by Western blot to evaluate the relative abundance of FLAG-atx3. Enrichment of lamin in the nuclear fractions was used as a control for the fractionation procedure. (C and D) For both expanded and nonexpanded forms of FLAG-atx3, densitometric analysis of the blots revealed that the phosphomutants have the same tendency for nuclear accumulation as their nonmutated counterparts (FLAG-atx3 22Q: $n = 3$ independent experiments; FLAG-atx3 84Q: five independent experiments; graph bars represent mean ± SEM; Kruskal-Wallis test: $P > 0.05$).

Provided online is the source code for Thresholderer, an ImageJ macro developed to analyze different immunofluorescence microscopy image parameters, including integrated signal density, at consecutive threshold levels.